

The Origin of Ripples in Cool Cores of Galaxy Clusters: Heating by MHD Waves?

Yutaka Fujita¹, Takeru K. Suzuki², Takahiro Kudoh³, and Takaaki Yokoyama⁴

ABSTRACT

We consider MHD waves as a heating source of cool cores of galaxy clusters. In particular, we focus on transverse waves (Alfvén waves), because they can propagate a longer distance than longitudinal waves (sound waves). Using MHD simulations, we found that the transverse waves can stably heat a cool core if the wave period is large enough ($\gtrsim 10^8$ yr). Moreover, the longitudinal waves that are created as a by-product of the nonlinear evolution of the transverse waves could be observed as the 'ripples' found in cool cores.

Subject headings: cooling flows — galaxies: active — galaxies: clusters: general — waves — X-rays: galaxies: clusters

1. Introduction

X-ray observations have shown that the radiative cooling time of the ICM (intracluster medium) in the central regions of galaxy clusters (cool cores) is generally smaller than the Hubble time. If there were no heating sources, the ICM flows subsonically toward the cluster center with a mass deposition rate of $\sim 100\text{--}1000 M_{\odot}\text{yr}^{-1}$ (Fabian 1994). This flow had been called a 'cooling flow'. However, recent X-ray observations have shown that the actual cooling rate of the ICM is much smaller. The Japanese *ASCA* (Advanced Satellite for Cosmology and Astrophysics) team indicated that metal emission lines from the low temperature cooling gas

¹Department of Earth and Space Science, Graduate School of Science, Osaka University, 1-1 Machikaneyama-cho, Toyonaka, Osaka 560-0043, Japan; fujita@vega.ess.sci.osaka-u.ac.jp

²Graduate School of Arts and Sciences, University of Tokyo, Komaba, Meguro, Tokyo 153-8902, Japan; stakeru@ea.c.u-tokyo.ac.jp

³Division of Theoretical Astronomy, National Astronomical Observatory of Japan, Mitaka, Tokyo 181-8588, Japan; kudoh@th.nao.ac.jp

⁴Department of Earth and Planetary Science, University of Tokyo, Hongo, Bunkyo, Tokyo, 113-0033, Japan; yokoyama.t@eps.s.u-tokyo.ac.jp

were much weaker than had been predicted by the classical cooling flow model (Ikebe et al. 1997; Makishima et al. 2001). This has been confirmed by *XMM-Newton* (Peterson et al. 2001; Kaastra et al. 2001; Tamura et al. 2001); the actual mass deposition rate is at least 5 or 10 times less than that previously assumed.

The lack of the cooling flows indicates that there are heating sources in the central regions of clusters that prevent the development of cooling flows. Most popular candidate of the heating source is AGNs at the centers of clusters. However, although the energy released by the AGNs is sufficient to cancel radiative cooling of the ICM in cool cores, the mechanism of energy transfer from the AGNs to the surrounding ICM is not clear. One possible mechanism is the dissipation of sound waves and weak shocks that have evolved from sound waves (Fabian et al. 2003; Ruszkowski et al. 2004; Fabian et al. 2005). Those waves could be generated by the activities of the central AGNs of clusters. In fact, sound waves and weak shocks are observed in the central regions of the Perseus and the Virgo Clusters (Fabian et al. 2003; Forman et al. 2005).

However, it has been shown that sound waves (longitudinal waves) and weak shocks that have evolved from the sound waves cannot stably heat a cool core, because they should dissipate before they propagate in the whole core. In other words, their dissipation length is too small. Even if their net energy is large enough to balance radiative cooling, the temperature profile of a cluster soon becomes irregular, which is not consistent with observations (Fujita & Suzuki 2005; Mathews et al. 2006). On the other hand, it seems to be curious that structures that look like sound waves ('ripples') have been observed far away ($r \sim 50$ kpc) from the central AGN in the Perseus cluster (Fabian et al. 2006). Since the dissipation length of the waves is small, the density fluctuations or the ripples should not be observed there if they were created at the cluster center.

So far, only longitudinal waves have been considered as heating sources in clusters. However, since the ICM is magnetized ($\sim 5\text{--}10 \mu\text{G}$; Clarke, Kronberg, & Böhringer 2001), there should be magnetohydrodynamic (MHD) waves including transverse waves. It has been known that transverse waves (Alfvén waves) can propagate a longer distance than longitudinal waves (e.g Suzuki 2002). Thus, the transverse waves could heat the whole core. In this letter, we consider the heating by transverse waves and longitudinal waves that are a by-product of nonlinear evolution of the transverse waves. The longitudinal waves could be observed as the ripples. We do not restrict the wave generators only to AGNs, because a long wave period is required to reproduce the ripples as shown below. It is to be noted that Makishima et al. (2001) proposed a heating model of MHD effects, but they considered magnetic reconnection instead of waves.

2. Models

The models presented here are based on heating models of the solar corona (Kudoh & Shibata 1999; Suzuki & Inutsuka 2005). We study the propagation of waves along a magnetic field line extending from the cluster center in the radial direction. We assume axisymmetry about this field line. In the vicinity of the line, we consider a local orthogonal curvilinear coordinate system defined by r , the distance from the cluster center, by the azimuthal angle θ measured about the axis of symmetry, and by ξ measured in the direction perpendicular to both r and θ vectors (Hollweg, Jackson, & Galloway 1982). In the following, the indices, r , θ , and ξ , indicate the vector components for each direction.

We assume ideal MHD (inviscid, perfect conductor) in a whole region:

$$\frac{\partial}{\partial t}(\rho S) + \frac{\partial}{\partial r}(\rho v_r S) = 0, \quad (1)$$

$$\frac{\partial}{\partial t}(\rho v_r S) + \frac{\partial}{\partial r} \left[\left(\rho v_r^2 + p + \frac{B_\theta^2}{8\pi} \right) S \right] = \rho \left[g_r + \left(v_\theta^2 - \frac{B_\theta^2}{4\pi\rho} \right) \frac{1}{R} \frac{dR}{dr} \right] S + \left(p + \frac{B_\theta^2}{8\pi} \right) \frac{dS}{dr}, \quad (2)$$

$$\frac{\partial}{\partial t}(\rho v_\theta R S) + \frac{\partial}{\partial r} \left[\left(\rho v_r v_\theta - \frac{B_r B_\theta}{4\pi} \right) R S \right] = 0, \quad (3)$$

$$\frac{\partial}{\partial t} \left(\frac{B_\theta S}{R} \right) - \frac{\partial}{\partial r} \left(\frac{E_\xi S}{R} \right) = 0, \quad (4)$$

$$\frac{\partial}{\partial t} \left[\left(\frac{p}{\gamma - 1} + \frac{1}{2} \rho v^2 + \frac{B_\theta^2}{8\pi} \right) S \right] + \frac{\partial}{\partial r} \left[\left(\left(\frac{\gamma}{\gamma - 1} p + \frac{1}{2} \rho v^2 \right) v_r - \frac{B_\theta E_\xi}{4\pi} \right) S \right] = (\rho g_r v_r - L) S, \quad (5)$$

$$E_\xi = -v_r B_\theta + v_\theta B_r, \quad (6)$$

$$v^2 = v_r^2 + v_\theta^2, \quad (7)$$

where ρ is the ICM density, S is the cross section of the magnetic flux tube, v is the velocity, p is the pressure, B is the magnetic field, R is the distance from the axis of the symmetry, E is the electric field, $\gamma (= 5/3)$ is the adiabatic index, g is the gravitational acceleration, and L is the cooling rate. We assumed that $\partial/\partial\theta = 0$, $v_\xi = 0$, and $B_\xi = 0$ in order to reduce the problem to one-dimension (Hollweg et al. 1982). For the sake of simplicity, we assume that the cluster is spherically symmetric, which means $S \propto r^{-2}$. The initial magnetic field is given by $B_r \propto r^{-2}$ and $B_\theta = 0$. We set the inner and outer boundaries at $r_{\text{in}} = 5$ kpc and $r_{\text{out}} = 84$ Mpc, respectively. Because of the large outer boundary, we do not have to consider the reflection of waves there. We adopted the relatively large inner radius to avoid the divergence of B_r at the cluster center. The beta parameter of the plasma is set to be one at $r = r_{\text{in}}$. Thus, for $r > r_{\text{in}}$ it increases rapidly as r increases, which means that the Alfvén velocity v_A is smaller than the sound velocity c_s . At $r = 20$ kpc, we obtain $B_r = 6 \mu\text{G}$.

Transverse waves are injected around the inner boundary in a form of acceleration in the θ direction. The wave acceleration is given by

$$A_w(t, r) = ag_{\text{in}} \exp \left[-\frac{1}{2} \left(\frac{r - r_{\text{in}}}{r_{\text{in}}} \right)^2 \right] \frac{\pi}{2} \sin \left(\frac{2\pi t}{P} \right), \quad (8)$$

where g_{in} is the gravitational acceleration from the cluster potential at $r = r_{\text{in}}$, and a and P are the parameters. Longitudinal waves are not injected for simplicity. It is to be noted that even if we give longitudinal waves with the same acceleration as that of the transverse waves, the resultant gas velocity of the longitudinal waves (v_r) is much smaller than that of the transverse waves (v_θ). This is because of the pressure gradient of the cluster, which prevents the ICM from being lifted in the r -direction.

We adopt a cooling function based on the detailed calculations by Sutherland & Dopita (1993),

$$L = n_e^2 \Lambda = [C_1(k_B T)^\alpha + C_2(k_B T)^\beta + C_3] n_i n_e, \quad (9)$$

where n_e and n_i are the electron and the ion number densities, respectively, and the units for $k_B T$ are keV. For an average metallicity $Z = 0.3 Z_\odot$, the constants in equation (9) are $\alpha = -1.7$, $\beta = 0.5$, $C_1 = 8.6 \times 10^{-3}$, $C_2 = 5.8 \times 10^{-2}$, and $C_3 = 6.4 \times 10^{-2}$, and we can approximate $n_i n_e = 0.70 (\rho/m_H)^2$, where m_H is the hydrogen mass. The units of Λ are 10^{-22} ergs cm^3 (Ruszkowski & Begelman 2002).

The model cluster we considered is similar to that adopted in § 3.2 of Fujita, Suzuki, & Wada (2004). The mass density profile of the cluster is given by the NFW profile (Navarro, Frenk, & White 1997). The viral mass is $1.2 \times 10^{15} M_\odot$, the concentration parameter is 4.7, and the characteristic radius is 460 kpc. For this cluster, $g_{\text{in}} = 1300 \text{kms}^{-1} (10^8 \text{yr})^{-1}$, which is a factor of two larger than the acceleration observed at the cold front in A1795 (Markevitch, Vikhlinin, & Mazzotta 2001). Initially, the cluster is isothermal and the temperature is 7 keV. The initial electron density at the cluster center is $n_{e0} = 0.017 \text{cm}^{-3}$. All of the calculations presented in this letter use CANS (Coordinated Astronomical Numerical Software)¹. The number of grid points is 16392. The grid size is 8.3 pc for $r < 120$ kpc and it increases logarithmically for $r > 120$ kpc.

3. Results

First, we investigate the case where waves are not injected for comparison (a genuine cooling flow). Fig. 1 shows the evolution of temperature and electron number density as

¹<http://www-space.eps.s.u-tokyo.ac.jp/%7Eyokoyama/etc/cans/index-e.html>

functions of distance from the cluster center. The interval of the lines is 0.8 Gyr. Because of radiative cooling, the temperature decreases and the density increases monotonically at the cluster center.

Next, we consider the heating by Alfvén waves by injecting transverse waves at the inner boundary. We take $a = 1$ and $P = 0.5$ Gyr. For this wave period P , the wave length of the sound waves is $c_s P \sim 700$ kpc. On the other hand, the wave length of the Alfvén waves is smaller and is $v_A P \sim 10$ kpc at $r \sim 20\text{--}50$ kpc, which is comparable to the observed wave length of ripples (Fabian et al. 2006). This wave period may be too large to be attributed to the activities of the central AGN; it could be attributed to gas motion around the central galaxy induced by minor cluster mergers such as ‘sloshing’ (Markevitch et al. 2001) or ‘tsunami’ (Fujita, Matsumoto, & Wada 2004). The wave injection in a form of acceleration (eq. [8]) would be preferable to model the waves of this kind, because the acceleration is independent of the gas flow toward the cluster center and the AGN. The transverse waves would be generated on the side of the sloshing central galaxy, but not in front and in the rear.

Fig. 2 shows the evolution of the temperature and density profiles when transverse waves are considered. We found that while the temperature at the cluster center decreases for $t \lesssim 4$ Gyr, it is stable and almost constant for $t \gtrsim 4$ Gyr until we stopped the calculation at $t = 6$ Gyr. Since we inject waves in a form of acceleration irrelevant of the gas mass of the core, the wave energy increases as the gas density in the core and thus the gas mass of the core increases. This is because for a given acceleration, the heavier the gas core is, the larger kinetic energy is given to the gas core. This is one reason that the temperature stops decreasing. The wave energy flux per unit area is given by $F_A = \rho v_\theta^2 (v_A + v_r) + v_r B_\theta^2 / (8\pi)$. At $r = 15$ kpc (outside the wave injection region), the energy flux is $4\pi r^2 F_A \sim 10^{42}$ erg s⁻¹ at $t \sim 0$, and it increases to $\sim 10^{44}$ erg s⁻¹ at $t \sim 6$ Gyr. Numerical simulations showed that the energy can be supplied by minor cluster mergers (Tittley & Henriksen 2005).

Fig. 3 shows the longitudinal and transverse velocity profiles at $t = 1.6$ and 3.2 Gyr. The transverse waves have reached $r = 57$ kpc at $t = 1.6$ Gyr and $r = 66$ kpc at $t = 3.2$ Gyr. In Fig. 3b, sharp jumps are seen; these jumps are formed through the steeping of Alfvén waves and are called ‘Switch-on shocks’ (e.g. Hollweg 1982; Suzuki 2004). At these shocks, while entropy is generated, longitudinal waves are also generated through nonlinear coupling (e.g. Hollweg 1992; Kudoh & Shibata 1999; Suzuki 2002; Suzuki & Inutsuka 2005). The longitudinal waves (sound waves) soon steepen and turn into weak shocks (N-waves; Fig. 3a), which also contribute to the heating of the ICM. Note that v_r is much smaller than v_θ . Contrary to the transverse waves, the longitudinal waves can be observed in temperature and density profiles. The temperature and density fluctuations seen in Fig. 2 reflect the

generation of the longitudinal waves. In particular, the density fluctuations could be observed as ripples. Since these longitudinal waves are generated away from the cluster center, they can be observed even at $r > 50$ kpc (Fig. 2b).

We also studied the mass inflow rate at the inner boundary. In the cooling flow case (Fig. 1), the inflow rate at $t = 4.8$ Gyr is $\dot{M} = 220 M_{\odot} \text{ yr}^{-1}$, and it is $310 M_{\odot} \text{ yr}^{-1}$ at $t = 6$ Gyr. On the other hand, waves can decrease the inflow rate significantly. In the case of Fig. 2, it is $\dot{M} = 60 M_{\odot} \text{ yr}^{-1}$ at $t \sim 4.8$ Gyr, which means that the waves effectively heat the surrounding ICM, although they cannot completely shut down a cooling flow. The inflow rate gradually increases, but even at $t \sim 6$ Gyr, it is still $\dot{M} = 80 M_{\odot} \text{ yr}^{-1}$.

We found that the heating by the Alfvén waves is fairly stable even if we change the acceleration parameter a , because as we mentioned above, high density coming from radiative cooling results in a high heating rate, and vice versa. Fig. 4 shows the results when $a = 2$ and $P = 0.5$ Gyr. Although the central temperature at which it stops decreasing (~ 4 keV; Fig. 4a) is higher than that in the case of $a = 1$ (~ 2 keV; Fig. 2a), the heating balances cooling after $t \sim 4$ Gyr. However, if a is much smaller than one, the waves cannot prevent the development of a cooling flow. In summary, a must be tuned to be ~ 1 – 2 in order to reproduce observed temperature profiles.

Moreover, we have investigated the heating by Alfvén waves with a relatively small wave period ($P \sim 10^7$ yr), which would be appropriate for waves generated by the activities of the central AGN. We found that the heating by these waves is not stable. The reason is similar to the heating by sound waves alone, that is, the waves can heat only the innermost region of the cluster.

4. Summary and Discussion

We have shown that Alfvén waves (transverse waves) with a long wave period can effectively heat cool cores of galaxy clusters. Since the dissipation rate of the waves is small, the waves can reach the outer core and then heat the whole core before they dissipate. During the propagation, sound waves (longitudinal waves) are generated through nonlinear coupling, and they would be observed as ripples. The long dissipation length indicates the superiority of the heating by the Alfvén waves over that by sound waves alone. In real clusters, however, it would be possible that sound waves created by AGN activities heat the inner cores, while Alfvén waves induced by cluster mergers heat the outer cores. In this case, the wave acceleration (A_w) required to heat the cores will be much smaller than that we assumed. We assumed that the Alfvén waves are generated close to the cluster center

($r \sim 5\text{--}10$ kpc). Fujita et al. (2004) showed that complex gas motion should be created even at the cluster center by minor cluster mergers. Thus, our assumption may be justified. However, if the waves are generated at some distance from the center, another heating source is required to heat the center.

In this letter, we considered only spherically symmetric magnetic fields. If they are not spherically symmetric, the heating should spatially be biased. In the region with stronger magnetic fields, Alfvén waves propagate faster and the heating is more effective. This could result in multiphase gas observed in the Perseus cluster (Fabian et al. 2006). If the longevity of optical filaments observed in the Perseus cluster (Conselice, Gallagher, & Wyse 2001) is smaller than the wave period, the filaments would indicate the direction of the wave oscillation or the motion of the central galaxy relative to the surrounding ICM. That is, the waves would be propagating in the direction perpendicular to the optical filaments. The model presented here predicts relatively large transverse velocity fluctuations (Fig. 3b), which could be detected in near-future space X-ray missions such as *NeXT*.

Y. F. and T. K. S. were supported in part by a Grant-in-Aid from the Ministry of Education, Culture, Sports, Science, and Technology of Japan (Y. F.: 17740162; T. K. S. 1884009).

REFERENCES

- Clarke, T. E., Kronberg, P. P., Böhringer, H. 2001, *ApJ*, 547, L111
- Conselice, C. J., Gallagher, J. S., III, & Wyse, R. F. G. 2001, *AJ*, 122, 2281
- Fabian, A. C. 1994, *ARA&A*, 32, 277
- Fabian, A. C., Reynolds, C. S., Taylor, G. B., & Dunn, R. J. H. 2005, *MNRAS*, 363, 891
- Fabian, A. C., Sanders, J. S., Allen, S. W., Crawford, C. S., Iwasawa, K., Johnstone, R. M., Schmidt, R. W., & Taylor, G. B. 2003, *MNRAS*, 344, L43
- Fabian, A. C., Sanders, J. S., Taylor, G. B., Allen, S. W., Crawford, C. S., Johnstone, R. M., & Iwasawa, K. 2006, *MNRAS*, 366, 417
- Forman, W., et al. 2005, *ApJ*, 635, 894
- Fujita, Y., Matsumoto, T., & Wada, K. 2004, *ApJ*, 612, L9
- Fujita, Y., & Suzuki, T. K. 2005, *ApJ*, 630, L1

- Fujita, Y., Suzuki, T. K., & Wada, K. 2004, *ApJ*, 600, 650
- Hollweg, J. V. 1982, *ApJ*, 254, 806
- Hollweg, J. V. 1992, *ApJ*, 389, 731
- Hollweg, J. V., Jackson, S., & Galloway, D. 1982, *Sol. Phys.*, 75, 35
- Ikebe, Y., et al. 1997, *ApJ*, 481, 660
- Kaasra, J. S., Ferrigno, C., Tamura, T., Paerels, F. B. S., Peterson, J. R., & Mittaz, J. P. D. 2001, *A&A*, 365, L99
- Kudoh, T., & Shibata, K. 1999, *ApJ*, 514, 493
- Makishima, K., et al. 2001, *PASJ*, 53, 401
- Markevitch, M., Vikhlinin, A., & Mazzotta, P. 2001, *ApJ*, 562, L153
- Mathews, W. G., Faltenbacher, A., & Brighenti, F. 2006, *ApJ*, 638, 659
- Navarro, J. F., Frenk, C. S., & White, S. D. M. 1997, *ApJ*, 490, 493
- Peterson, J. R., et al. 2001, *A&A*, 365, L104
- Ruszkowski, M. & Begelman, M. C. 2002, *ApJ*, 581, 223
- Ruszkowski, M., Brüggén, M., & Begelman, M. C. 2004, *ApJ*, 615, 675
- Sutherland, R. S. & Dopita, M. A. 1993, *ApJS*, 88, 253
- Suzuki, T. K. 2002, *ApJ*, 578, 598
- Suzuki, T. K. 2004, *MNRAS*, 349, 1227
- Suzuki, T. K., & Inutsuka, S. 2005, *ApJ*, 632, L49
- Tamura, T., et al. 2001, *A&A*, 365, L87
- Tittley, E. R., & Henriksen, M. 2005, *ApJ*, 618, 227

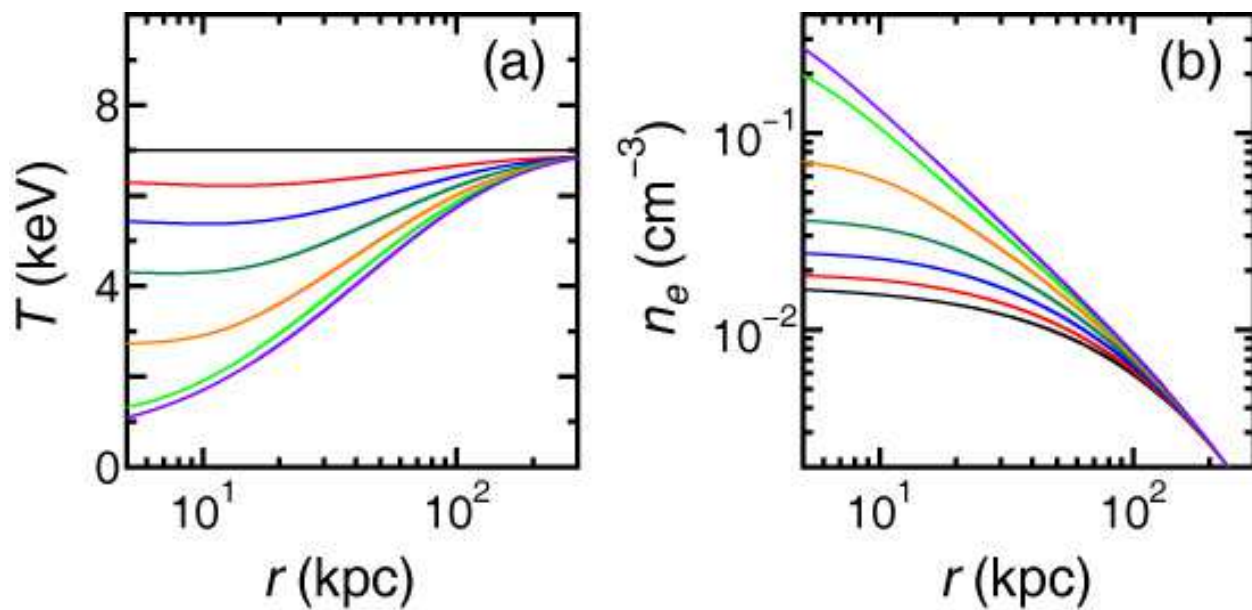


Fig. 1.— Time sequence of temperature and electron number density for $a = 0$. They are shown every 0.8 Gyr

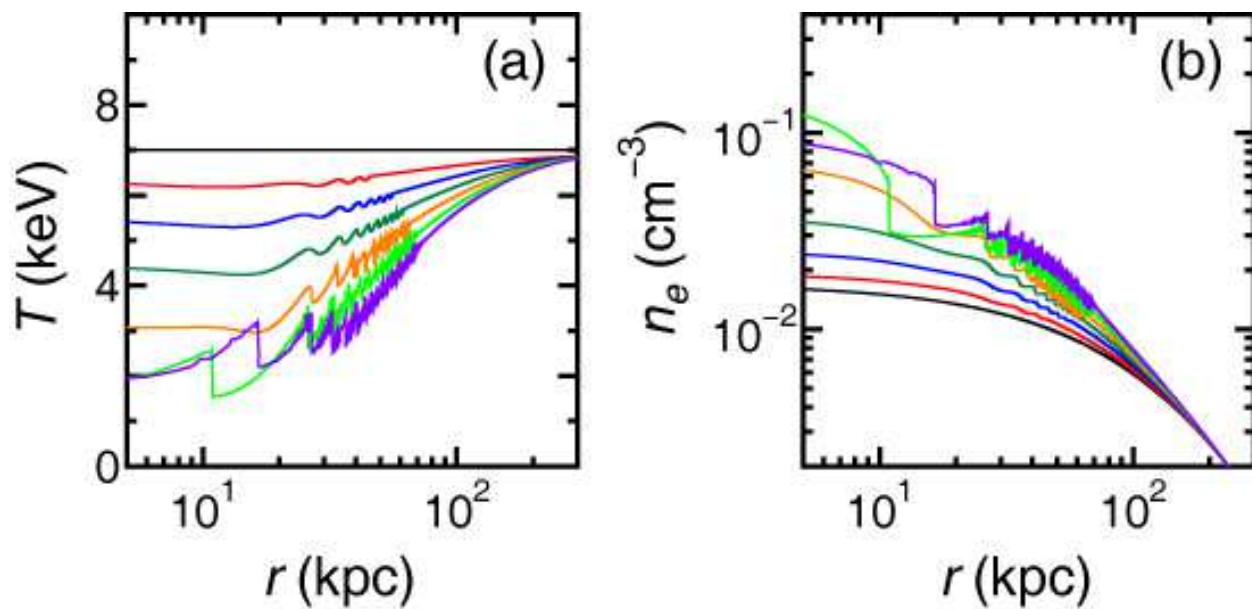


Fig. 2.— Same as Fig. 1, but for $a = 1$ and $P = 0.5$ Gyr.

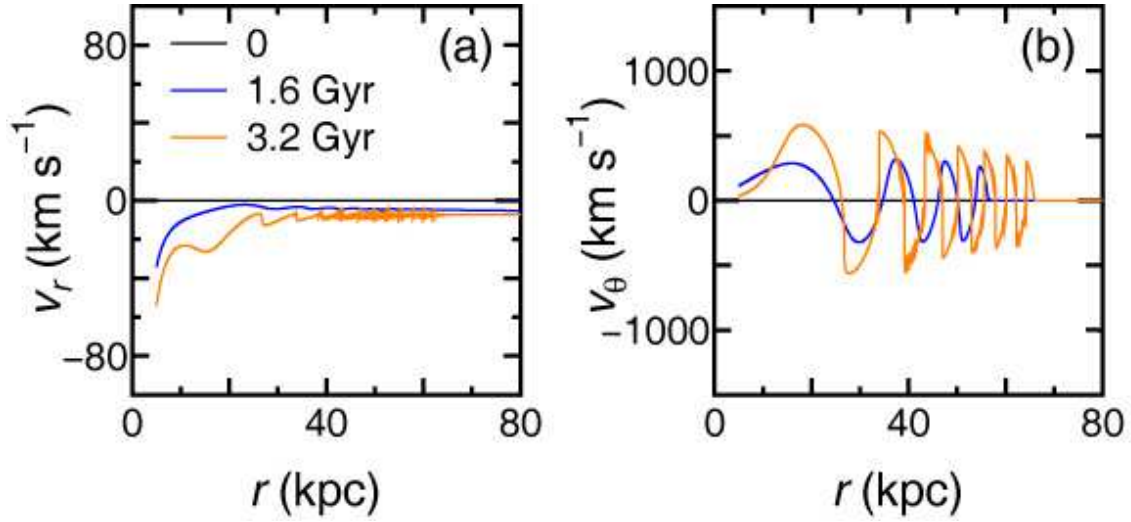


Fig. 3.— The longitudinal (v_r) and transverse (v_θ) velocity profiles at $t = 1.6$ and 3.2 Gyr. Note that the scales of the vertical axes are different.

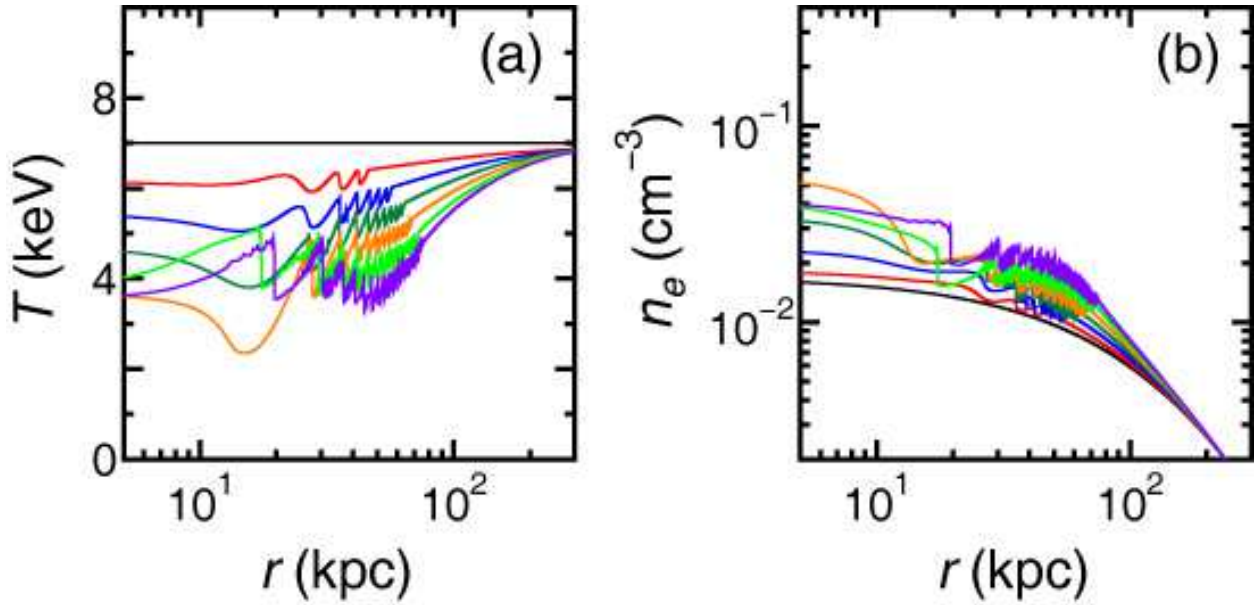


Fig. 4.— Same as Fig. 1, but for $a = 2$ and $P = 0.5$ Gyr.